HIGHER ORDER 1-D FDTD SEISMIC MODELLING USING THE STAGGERED ADAMS-BASHFORTH TIME INTEGRATOR

T. Bohlen and F. Wittkamp

email: *thomas.bohlen@kit.edu*

keywords: *seismic modelling, higher order finite difference, time discretization, Adams-Bashforth method*

ABSTRACT

We analyze the performance of a higher order accurate staggered Finite-Difference Time Domain (FDTD) method, in which the Adams-Bashforth third-order (M=3) and fourth-order (M=4) accurate time integrators are used for temporal discretization. The analysis shows that the numerical dispersion is much lower than that of the widely used second-order leapfrog method. Numerical dissipation is introduced by the ABS method which is significantly smaller for the ABS method of fourth-order accuracy. The ABS method does not require much additional floating point operations but the additional storage of M-1 perviously calculated time-levels of spatial derivative wave fields. In a 1-D simulation experiment we verify the convincing improvements of simulation accuracy of the fourth-order ABS method which is straightforward to implement in 2-D and 3-D FDTD simulation codes.

INTRODUCTION

Today, full wavefield seismic imaging and full waveform inversion require the efficient and accurate numerical simulation of seismic waves through complex earth models. For this purpose also higher-order Finite-difference (FD) methods are widely applied where the wave equation is discretized in both space and time. For the spatial derivatives many different methods are available, e.g. pseudo-spectral methods or high-order centered FD approximations. For the time discretization, however, the second order FD leapfrog scheme is still common because of its easy implementation and zero requirements of computer memory. More recently, new techniques have been proposed that allow to increase the order of time discretization without significantly increasing the memory requirements. The most popular strategy today is the so-called Lax-Wendroff method which replaces high-order temporal derivatives in the Taylor series expansion by spatial derivatives using the wave equation (Dablain (1986); Blanch and Robertsson (1997)). However, in 2D and 3D media the Lax-Wendroff approach involves quite expensive calculations of high-order mixed spatial derivatives and thus leads to an increase of floating point operations on extended spatial stencils. Recently, Tan & Huang (2014) developed an shorter Lax-Wendroff-type stencil having only a few more grid points and floating point operations than the standard stencil.

Another approach to increase the temporal accuracy is the predictor-corrector optimally accurate FD scheme of Geller & Takeuchi (1998). This scheme is essentially equivalent to a Lax-Wendroff scheme with fourth-order accuracy in both space and time.

Liu & Sen (2009) achieved higher order accuracy in time by minimizing the dispersion relations in the joint time-space domain. Their scheme yields higher order accuracy in 2D along eight spatial directions only. More recently, Liu & Sen (2013) improved this scheme to higher order accuracy for all spatial direction using a spatially extended rhombus-shaped stencil. Both the commonly applied Lax-Wendroff methods (Dablain, 1986; Tan and Huang, 2014) and the joint time-space discretization of Liu & Sen (2013) require spatially extended stencils which can lead to simulation errors in case of strong material discontinuities (Tan and Huang, 2014).

A different strategy to increase the temporal accuracy are multi-step methods (Hairer et al., 2006). In a multi-step method the history of the temporal evolution is stored to increase the order of the time integration. The classical way are Runge-Kutta methods that yield better accuracy for long-time simulations than the Lax-Wendroff schemes (Chen, 2007). Ghrist et al. (2000) compare two other multi-step methods, the Adams-Bashforth (ABS) and the Backward Differentiation method (BDS) which are more appropriate for wave equations. They show that the numerical dispersion of both methods is similar but the stability restraint of the ABS method is much relaxed by approximately 33 per cent. Furthermore, the BDS method is stable for wave equation simulations up to fourth order only, whereas the ABS method is stable also for higher orders.

In this work we further investigate the numerical properties of the more stable staggered Adams-Bashforth method towards the future implementation into 3-D forward and full waveform inversion schemes (Bohlen, 2002; Butzer et al., 2013). The ABS method has the following important advantages over the other methods discussed above. (1) The ABS method has a relatively large region of stability. (2) Its implementation is straightforward. (3) The time discretization is independent of the used spatial discretization scheme. (4) The additional computational costs (floating point operations) are negligible. The main and perhaps only disadvantage is an increase of the memory requirements due to the storage of previous time levels of wavefield. This seems to be affordable on modern and future parallel computing architectures.

ADAMS-BASHFORTH METHOD ON TIME STAGGERED GRIDS

In order to illustrate the staggered Adams-Bashforth method (ABS-method) we consider the 1-D acoustic wave equation in velocity-stress formulation

$$\frac{\partial p(x,t)}{\partial t} = -K(x)\frac{\partial v(x,t)}{\partial x} \quad , \quad \frac{\partial v(x,t)}{\partial t} = -\rho^{-1}(x)\frac{\partial p(x,t)}{\partial x} \tag{1}$$

The wavefield variables are the pressure $p(x,t)$ and the particle velocity $v(x,t)$. The material is described by the modulus $K(x)$ and the mass density $\rho(x)$. For simplicity we omit the temporal and spatial dependencies in the following.

Using the conventional second order staggered grid approximation to the first order time derivative we obtain

$$\frac{p|^{n+1/2} - p|^{n-1/2}}{\triangle t} = -K\frac{\partial v}{\partial x}\bigg|^{n} \quad , \quad \frac{v|^{n} - v|^{n-1}}{\triangle t} = -\rho^{-1}\frac{\partial p}{\partial x}\bigg|^{(n-1/2)} \tag{2}$$

This results in the conventional explicit second order accurate time-stepping (leapfrog) scheme

$$p|^{n+1/2} = p|^{n-1/2} - \triangle t K\frac{\partial v}{\partial x}\bigg|^{n} \quad , \quad v^{n} = v^{n-1} - \triangle t\rho^{-1}\frac{\partial p}{\partial x}\bigg|^{(n-1/2)} \tag{3}$$

which requires no additional storage of the wavefield variables p and v.

The order of the temporal integration can be increased by a multi-step method (Hairer et al., 2006; Ghrist et al., 2000). Ghrist et al. (2000) compare the Backward Differentiation method (BDS) and the Adams-Bashforth (ABS) method. The BDF method uses time levels of previous pressure field $p|^{n-3/2}, p|^{n-5/2}, ...$ and correspondingly particle velocity $v|^{n-2}, v|^{n-3}, ...$ This corresponds to a backward differentiation of the time derivatives on the left hand side of equations 1 and 2. The required weights can be found by a one-sided Taylor series expansion (Fornberg, 1988). The ABS method uses previous time levels of the right hand side of equation 2 instead. These are used in the following way:

$$p|^{n+1/2} = p|^{n-1/2} - \triangle t K\sum_{l=0}^{M-1} a_l\frac{\partial v}{\partial x}\bigg|^{n-l} \quad , \quad v|^{n} = v|^{n-1} - \triangle t\rho^{-1}\sum_{l=0}^{M-1} a_l\frac{\partial p}{\partial x}\bigg|^{(n-1/2-l)} \tag{4}$$

The weights for the accuracy orders $M = 2, 3, 4$ are given in Table 1. Ghrist et al. (2000) show that the numerical error due to dispersion and attenuation of the BDS and ABS method are comparable. The significant advantage of the ABS method over the BDS method is a greater region of stability allowing to choose greater Courandt numbers (time step intervals) by approximately 33 per cent and thus to reduce the total computation time considerably (Ghrist et al., 2000; Xiao et al., 2007).

1-D APPLICATION

Our aim is to explore the performance of the ABS method for realistic geophysical medium properties and long propagation distances. In our first scenario we test the explicit ABS staggered time-stepping scheme of equations 4 for a 1-D homogeneous acoustic medium having a wave velocity of $c = 500\,m/s$. The source excites a Ricker signal with a center frequency of 20 Hz. The dominant wavelength is thus 25 m. We choose a quite large source-receiver distance of 3000 m corresponding to 120 dominant wavelength to emphasize the effects of numerical dispersion and numerical damping in the synthetic seismograms. The spatial derivatives are always computed with a centered staggered FD stencil of 10th order accuracy. The spatial grid spacing is held constant at 2 m. The propagating waves are thus spatially discretized with approx. 12 grid points per dominant wavelength. This results in highly accurate calculations of spatial derivatives. The discrepancies to the analytical solution are thus mainly caused by the lower order temporal discretization of the ABS scheme where we compare the orders $M = 2, 3$ and 4. The numerical results for Courandt numbers CFL=0.4, 0.2, 0.1 and temporal orders of accuracy $M = 2, 3, 4$ are compared with the analytical solution in Figure 1. For a large time step interval (CFL=0.4) and second order approximation of the time derivative ($M = 2$) we can observe large time dispersion error indicated by a leading phase with high amplitude (Figure 1, top-left). Figure 1 compares two ways to reduce the time discretization error. The common way is to reduce the time step interval, i.e. Courandt number. This resulting waveforms are shown in the rows of Figure 1. Reducing the CFL-number will increase the computation time proportional to 1/CFL, i.e. The multi-step ABS method allows for a second strategy by using $M - 1$ previously calculated spatial derivates of the wavefield. The resulting waveforms are shown in the columns of Figure 1. Increasing the order M improves the simulation accuracy without significant computational cost but requires the storage of $M - 1$ additional time levels of the spatial derivative wavefields.

In order to quantify the numerical simulation error we compute the L2 misfit between the numerical and analytical solution for different Courandt numbers and accuracy orders $M = 2, 3, 4$. The results are shown in Figure 2 (left). As expected from the seismogram comparisons shown in Figure 1, we observe a significant improvement of the simulation accuracy if we increase the temporal accuracy order M. The additional computational costs are very small (Figure 2 (right)).

DISPERSION ANALYSIS

In order to calculate the dispersion relation we insert a plain wave into the discrete scheme 4. The plain wave is described by

$$p = p_0 \cdot e^{i(kx+\omega t)} \text{ and } v = v_0 \cdot e^{i(kx+\omega t)}, \tag{5}$$

which can be expressed in a discrete way as follow:

$$p_j^n = p_0 \cdot e^{i(kj\Delta x+\omega n\Delta t)} \text{ and } v_j^n = v_0 \cdot e^{i(kj\Delta x+\omega n\Delta t)}. \tag{6}$$

Thereby p_0 and v_0 are the amplitudes, k is the wave number and ω is the circular frequency. j and n are the spatial and temporal indices, respectively.

M	a_0	a_1	a_2	a_3
2	1	0	0	0
3	25/24	-1/12	1/24	0
4	13/12	-5/24	1/6	-1/24

Table 1: Weights used in equation 4 for the staggered approximation of the first time derivative using the Adams-Bashforth method (Ghrist et al. (2000)).

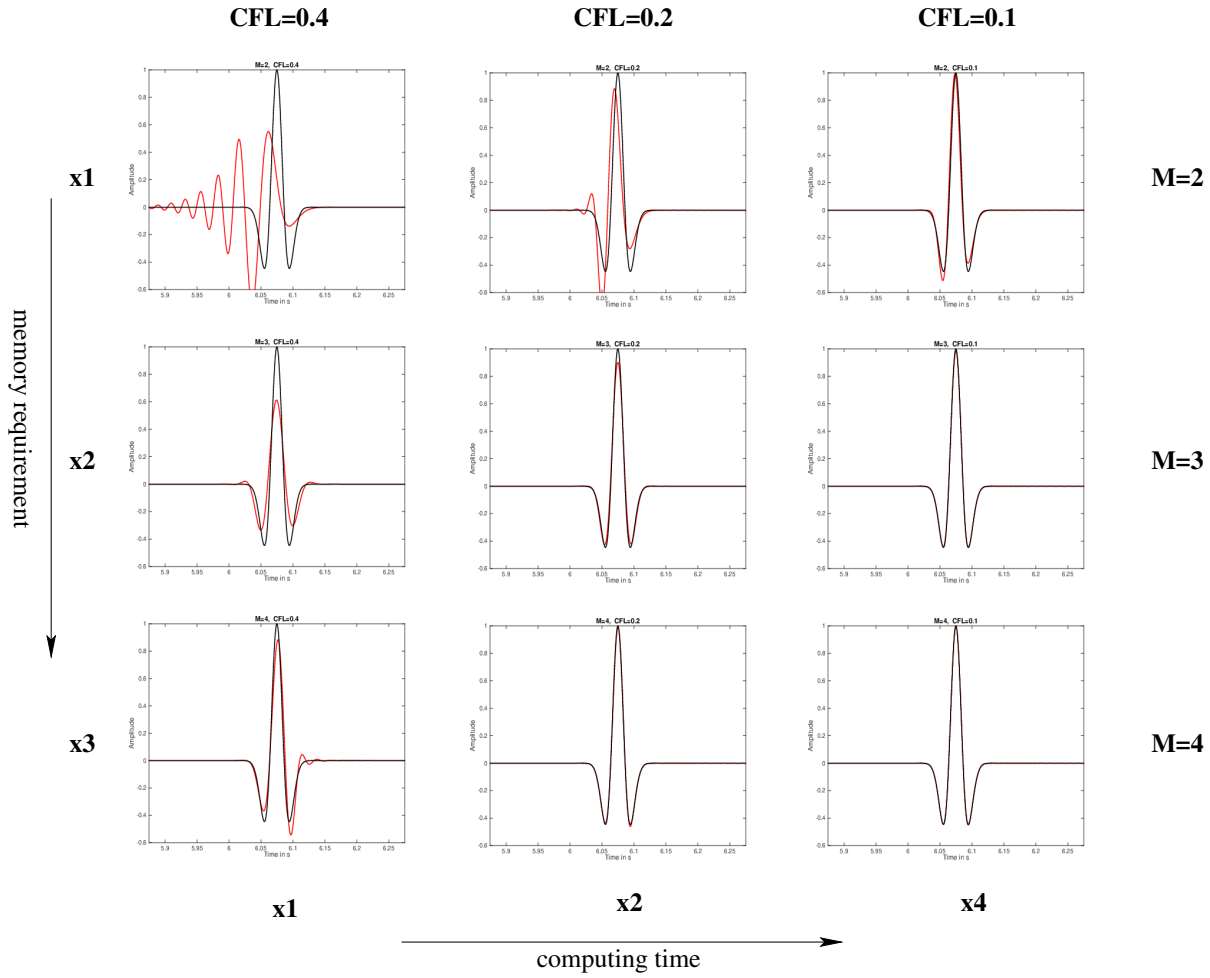

Figure 1: Seismograms calculated for the 1-D case via equations 4 for different Courandt numbers (CFL) and accuracy orders M. $M = 2$ corresponds to the classical second order leapfrog scheme. $M = 3, 4$ correspond to the multi-step ABS method. The analytical solution is plotted as a black line. The computing time is proportional to 1/CFL. The relative additional memory to save previous time levels is proportional to $M - 1$ (Table 1).

First we calculate the ratio between the amplitudes:

$$\frac{\partial}{\partial t} p_0 \cdot e^{i(kx+\omega t)} = -M \frac{\partial}{\partial x} v_0 \cdot e^{i(kx+\omega t)} \tag{7}$$

$$i \cdot p_0 \cdot \omega = -i \cdot v_0 \cdot M \cdot k \tag{8}$$

$$\Longrightarrow \frac{p_0}{v_0} = -\frac{M \cdot k}{\omega}. \tag{9}$$

Using the relation between the circular frequency and the wave number $\omega = k \cdot c$ we get:

$$\frac{p_0}{v_0} = -\frac{M}{c}. \tag{10}$$

Now we insert the ansatz of a discrete plain wave into the spatial derivatives. For simplicity we show

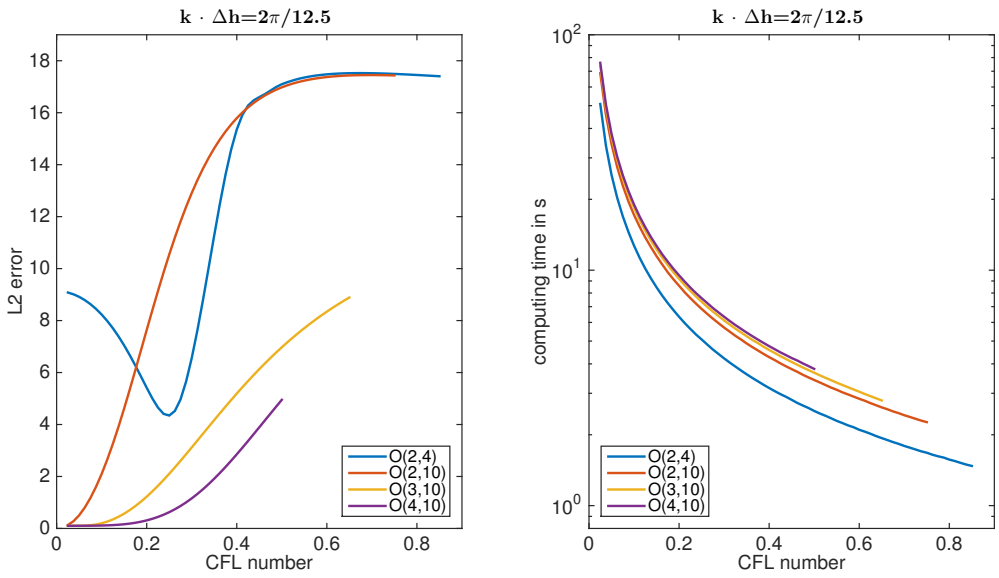

Figure 2: L2 numerical error (left) and calculation time (right) as a function of Courandt number (CFL) for the 1-D numerical experiment. Orders of temporal accuracy are $M = 2, 3, 4$. The spatial accuracy is of order 10. For comparison the behavior of the widely used $\mathcal{O}(2, 4)$-scheme is also shown.

the derivation exemplarily for spatial derivatives of fourth order accuracy.

$$\frac{\partial}{\partial x} v_j^n = \frac{9}{8 \cdot \Delta x} \left(v_{j+\frac{1}{2}}^n - v_{j-\frac{1}{2}}^n \right) - \frac{1}{24 \cdot \Delta x} \left(v_{j+\frac{3}{2}}^n - v_{j-\frac{3}{2}}^n \right) \tag{11}$$

$$= \frac{9 \cdot v_0 \cdot z(n)}{8 \cdot \Delta x} \left(e^{i\frac{1}{2}k\Delta x} - e^{-i\frac{1}{2}k\Delta x} \right) - \frac{1 \cdot v_0 \cdot z(n)}{24 \cdot \Delta x} \left(e^{i\frac{3}{2}k\Delta x} - e^{-i\frac{3}{2}k\Delta x} \right) \tag{12}$$

$$= \frac{2i \cdot v_0 \cdot z(n)}{\Delta x} \underbrace{\left(\frac{9}{8} \sin(\frac{k\Delta x}{2}) - \frac{1}{24} \sin(\frac{3k\Delta x}{2}) \right)}_{\beta} \tag{13}$$

$$= \frac{2i \cdot v_0 \cdot \beta}{\Delta x} \cdot z(n) \tag{14}$$

where the relation $2 \cdot i \cdot \sin(u) = e^{iu} - e^{-iu}$ and the shortcut $z(n) = e^{i(\omega n \Delta t + kj\Delta x)}$ is used.

Now we insert the discrete plain wave into equation 4 assuming $M = 4$.

$$2i \cdot p_0 \cdot z(n) \left(e^{i\frac{1}{2}\omega\Delta t} - e^{-i\frac{1}{2}\omega\Delta t} \right) =$$

$$-\frac{M_j \cdot \Delta t \cdot 2i \cdot v_0 \cdot \beta}{\Delta x} \left[\frac{13}{12} z(n) - \frac{5}{24} z(n-1) + \frac{1}{6} z(n-2) - \frac{1}{24} z(n-3) \right], \tag{15}$$

which is equal to:

$$z(n) \sin(\frac{\omega\Delta t}{2}) = -\frac{M_j \cdot \Delta t \cdot v_0 \cdot \beta}{\Delta x \cdot p_0} \left[\frac{13}{12} z(n) - \frac{5}{24} z(n-1) + \frac{1}{6} z(n-2) - \frac{1}{24} z(n-3) \right]. \tag{16}$$

Using the CFL number $r = \frac{c \cdot \Delta t}{\Delta x}$ we can write

$$\sin(\frac{\omega\Delta t}{2}) = r \cdot \beta \left[\frac{13}{12} - \frac{5}{24} e^{-i\omega\Delta t} + \frac{1}{6} e^{-2i\omega\Delta t} - \frac{1}{24} e^{-3i\omega\Delta t} \right] \tag{17}$$

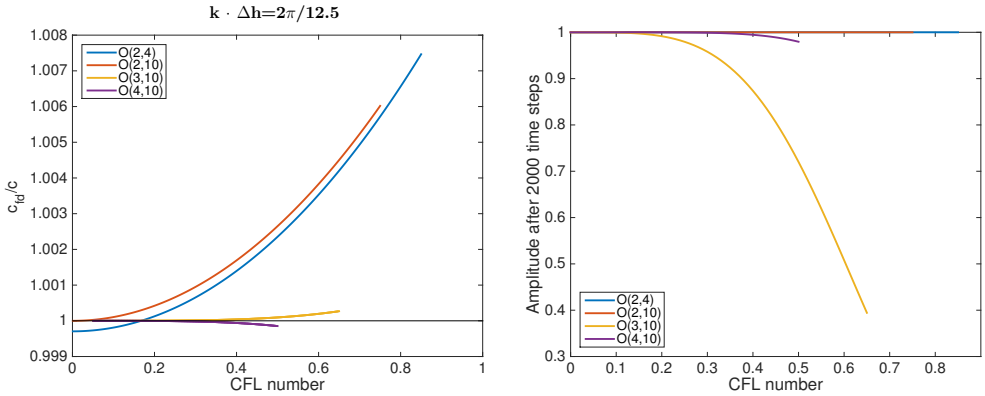

Figure 3: Numerical dispersion and dissipation caused by time discretization for the ABS scheme as a function of Courandt number (CFL). Temporal orders of accuracy of $M = 2, 3, 4$ are compared. For comparison we show the behavior of the widely used $\mathcal{O}(2, 4)$ scheme.

Insert $e^{-i\omega\Delta t} = \cos(\omega\Delta t) - i\sin(\omega\Delta t)$ in the equation above and extract the real part we get (below only the real part of the equation is shown):

$$\sin(\frac{\omega\Delta t}{2}) = r \cdot \beta \left[\frac{13}{12} - \frac{5}{24}\cos(\omega\Delta t) + \frac{1}{6}\cos(2\omega\Delta t) - \frac{1}{24}\cos(3\omega\Delta t)\right] \tag{18}$$

The velocity of the wave in the numerical model is $c_{\text{fd}} = \frac{\omega}{k}$. By taking the ratio between the numerical velocity and the physical velocity we find the dispersion relation:

$$\frac{c_{\text{fd}}}{c} = \frac{\frac{\omega}{k}}{c} = \frac{\frac{\omega}{k}}{\frac{r\cdot\Delta x}{\Delta t}} = \frac{\omega\Delta t}{k\cdot\Delta x\cdot r}. \tag{19}$$

We now rearrange equation 19 to $\omega\Delta t$ and substitute this in equation 18. So we obtain a implicit equation for the dispersion relation of a ABS4 finite difference scheme with fourth order in time:

$$\frac{\sin(\frac{1}{2}\frac{c_{\text{fd}}}{c}k\Delta x\cdot r)}{\frac{13}{12} - \frac{5}{24}\cos(\frac{c_{\text{fd}}}{c}k\Delta x\cdot r) + \frac{1}{6}\cos(2\frac{c_{\text{fd}}}{c}k\Delta x\cdot r) - \frac{1}{24}\cos(3\frac{c_{\text{fd}}}{c}k\Delta x\cdot r)} = r\cdot\beta \tag{20}$$

For the ABS3 finite difference scheme with third order in time we get:

$$\frac{\sin(\frac{1}{2}\frac{c_{\text{fd}}}{c}k\Delta x\cdot r)}{\frac{25}{24} - \frac{1}{12}\cos(\frac{c_{\text{fd}}}{c}k\Delta x\cdot r) + \frac{1}{24}\cos(2\frac{c_{\text{fd}}}{c}k\Delta x\cdot r)} = r\cdot\beta \tag{21}$$

The numerical dispersion of the spatial discretization is hidden in the factor β (see equation 14).

The numerical dispersion due to time discretization as a function of the CFL number for the given 1-D scenario is shown in Figure 3 (left). (The spatial dispersion error at the applied spatial sampling of 12.5 grid points per wavelength is small for the spatial order of accuracy of 10.) We see a significant reduction of the numerical time dispersion error when increasing the temporal order of accuracy ($M = 2, 3, 4$).

0.1 DISSIPATION ERROR

In contrast to the common leapfrog scheme (M=2), the ABS method (M>2) leads to a numerical amplitude loss with propagation distance called numerical dissipation. In order to quantify the numerical dissipation we follow the approach of Fei and Xiaohong (2006).

$$p_j^n = p_0 \cdot g^n \cdot e^{i\cdot j\cdot k\Delta x}\,, \tag{22}$$

$$v_j^n = v_0 \cdot g^n \cdot e^{i\cdot j\cdot k\Delta x} = -\frac{c}{M}\cdot p_0 \cdot g^n \cdot e^{i\cdot j\cdot k\Delta x}\,, \tag{23}$$

where the ratio of the amplitudes (equation 10) was used.
To start we insert the equations above in the spatial derivation of the velocity:

$$\frac{\partial}{\partial x} v_j^n = \frac{9}{8 \cdot \Delta x} \left(v_{j+\frac{1}{2}}^n - v_{j-\frac{1}{2}}^n \right) - \frac{1}{24 \cdot \Delta x} \left(v_{j+\frac{3}{2}}^n - v_{j-\frac{3}{2}}^n \right) \tag{24}$$

$$= -\frac{2i \cdot c \cdot p_0 \cdot g^n \cdot e^{i \cdot j \cdot k \Delta x}}{M \cdot \Delta x} \underbrace{\left(\frac{9}{8} \sin(\frac{k\Delta x}{2}) - \frac{1}{24} \sin(\frac{3 \cdot k\Delta x}{2}) \right)}_{\alpha(k\Delta x)} \tag{25}$$

$$= -\frac{2i \cdot c \cdot p_0 \cdot g^n \cdot e^{i \cdot j \cdot k \Delta x}}{M \cdot \Delta x} \cdot \alpha(k\Delta x) \tag{26}$$

Now we substitute the equations 22 and 23 in the explicit temporal fourth order update equations for the pressure and do some simplifications. We can write:

$$0 = g^{\frac{1}{2}} - g^{-\frac{1}{2}} - 2i \cdot r \cdot \alpha(k\Delta x) \left(\frac{13}{12} - \frac{5}{24} g^{-1} + \frac{1}{6} g^{-2} - \frac{1}{24} g^{-3} \right) \tag{27}$$

After a multiplication with g^3 we obtain the characteristic polynominal:

$$0 = g^{\frac{7}{2}} - g^{\frac{5}{2}} - 2i \cdot r \cdot \alpha(k\Delta x) \left(\frac{13}{12} g^3 - \frac{5}{24} g^2 + \frac{1}{6} g^1 - \frac{1}{24} \right) \tag{28}$$

For the ABS3 scheme with third order accuracy in time we would get:

$$0 = g^{\frac{5}{2}} - g^{\frac{3}{2}} - 2i \cdot r \cdot \alpha(k\Delta x) \left(\frac{25}{24} g^2 - \frac{1}{12} g^1 + \frac{1}{24} \right) \tag{29}$$

The classical leapfrog scheme will result in:

$$0 = g^{\frac{1}{2}} - g^{-\frac{1}{2}} - 2i \cdot r \cdot \alpha(k\Delta x) \tag{30}$$

According to Fei and Xiaohong (2006) we get the dissipation by $|g_i|$ where g_i is the root of the characteristic polynominal. The characteristic polynominal has high order terms regarding g, so it will be difficult to find analytical solutions. Therefore we used a numerical solver to obtain the solutions. In case the characteristic polynominal has more than one solution, we only considered the solution which is suitable to our problem.

We calculated the dissipation for the FD-schemes $\mathcal{O}(\Delta t^2, \Delta x^{10})$, $\mathcal{O}(\Delta t^3, \Delta x^{10})$ and $\mathcal{O}(\Delta t^4, \Delta x^{10})$ as a function of CFL numbers assuming the given 1-D scenario described above. The results are shown in Figure 3 (right). The classical leapfrog schemes ($M = 2$) are free of dissipation. Their numerical error is solely caused by numerical dispersion shown in Figure 3 (left).The ABS3 scheme ($M = 3$) experiences a quite significant dissipation, whereas the dissipation caused by the ABS4 scheme ($M = 4$) is significantly smaller. This is strong argument for using the ABS4 scheme instead of ABS3.

CONCLUSIONS

In this work we analyze the numerical properties of the Adams-Bashforth method to increase the temporal order of accuracy in staggered finite-difference seismic wave simulations. In a 1-D geophysical simulation experiment the ABS method of orders M=3 and 4 can improve the simulation accuracy with only slightly increased computation time compared to the commonly used leapfrog time stepping method (M=2). The ABS method requires additional storage of M-1 previously calculated time-levels of the spatial derivative wavefields. The implementation is straightforward and independent of the method to calculate the spatial wavefield derivatives. It can thus also be used for other time-stepping simulation methods such as pseudo-spectral, finite-element or discontinuous Galerkin methods. The future implementation into our 2-D and 3-D FDTD simulation codes will improve our simulation accuracy which is especially important for future full waveform inversion applications.

ACKNOWLEDGMENTS

This work is kindly supported by the sponsors of the *Wave Inversion Technology (WIT) Consortium*. We thank Marlis Hochbruck (KIT) and Christian Wieners (KIT) for the helpful discussions.

REFERENCES

Blanch, J. and Robertsson, J. (1997). A modified lax-wendroff correction for wave propagation in media described by zener elements. *Geophysical Journal International*, 131(2):381–386.

Bohlen, T. (2002). Parallel 3-d viscoelastic finite difference seismic modelling. *Computers & Geosciences*, 28(8):887 – 899.

Butzer, S., Kurzmann, A., and Bohlen, T. (2013). 3d elastic full-waveform inversion of small-scale heterogeneities in transmission geometry. *Geophysical Prospecting*, 61(6):1238–1251.

Chen, J.-B. (2007). High-order time discretizations in seismic modeling. *Geophysics*, 72(5):SM115–SM122.

Dablain, M. (1986). The application of high-order differencing to the scalar wave equation. *Geophysics*, 51:54–66.

Fei, X. and Xiaohong, T. (2006). Stability and numerical dispersion analysis of a fourth-order accurate fdtd method. *Antennas and Propagation, IEEE Transactions on*, 54(9):2525–2530.

Fornberg, B. (1988). Generation of finite difference formulas on arbitrarily spaced grids. *Mathematics of computation*, 51(184):699–706.

Geller, R. J. and Takeuchi, N. (1998). Optimally accurate second-order time-domain finite difference scheme for the elastic equation of motion: one-dimensional cases. *Geophysical Journal International*, 135(1):48–62.

Ghrist, M., Fornberg, B., and Driscoll, T. A. (2000). Staggered time integrators for wave equations. *SIAM Journal on Numerical Analysis*, 38(3):718–741.

Hairer, E., Nørsett, S., and Wanner, G. (2006). *Solving ordinary differential equations*. Springer.

Liu, Y. and Sen, M. K. (2009). A new time–space domain high-order finite-difference method for the acoustic wave equation. *Journal of computational Physics*, 228(23):8779–8806.

Liu, Y. and Sen, M. K. (2013). Time-space domain dispersion-relation-based finite-difference method with arbitrary even-order accuracy for the 2d acoustic wave equation. *J. Comput. Phys.*, 232(1):327–345.

Tan, S. and Huang, L. (2014). An efficient finite-difference method with high-order accuracy in both time and space domains for modelling scalar-wave propagation. *Geophysical Journal International*.

Xiao, F., Tang, X., and Wang, L. (2007). An explicit fourth-order accurate fdtd method based on the staggered adams-bashforth time integrator. *Microwave and Optical Technology Letters*, 49(4):910–912.